International Journal of Engineering & Technology, 7 (4.39) (2018) 308-313

International Journal of Engineering & Technology

Website: www.sciencepubco.com/index.php/IJET

Research paper

Optimization of Process Parameters during TIG Welding of 304L Stainless Steel with and without Flux

Md Suraj[1], S. Tripathy[2], N. Pallavi Senapati[3*]

[1]*M. Tech student, Dept. of Mechanical Engineering, ITER, Siksha 'O' Anusandhan (Deemed to be University), Bhubaneswar, India.*
[2]*Associate Professor, Dept. of Mechanical Engineering, ITER, Siksha 'O' Anusandhan (Deemed to be University), Bhubaneswar, India.*
[3]*Research Scholar, Dept. of Mechanical Engineering, ITER, Siksha 'O' Anusandhan (Deemed to be University), Bhubaneswar, India.*
**Corresponding author E-mail: sasmeetatripathy@soa.ac.in*

Abstract

The aim of this experimental study is to investigate the welding performance of 304L stainless steel by tungsten inert gas (TIG) welding process. SiO_2 and $CdCl_2$ were used as fluxes for welding using activated flux (A-TIG) and the influence of machining factors on the welding responses of 304L stainless steel were compared and studied. The experimental design was carried out using Taguchi's technique where L_{27} orthogonal array was used for welding. Multi-objective optimization was carried out using PCA based TOPSIS method to find the optimal sample among the entire samples. The optimal sample was found to be SiO_2 flux at welding current=160 A, gas flow rate=16l/min and weight of the flux=0.147g.

Keywords: *A-TIG welding; activated fluxes; Chlorides; oxides*

1. Introduction

TIG welding is used in those applications where the shape of the weld bead and the metallurgical properties of the material are necessary to be controlled. But this technique has low productivity, especially during the joining of larger components. It can weld carbon steel, stainless steel plates of about 2–3 mm thickness within Argon gas shielding in autogenous mode. To overcome these limitations, TIG welding using activated flux (A-TIG welding) method was invented in the Paton welding Institute during the 1960s and is regarded as a reasonable alternate method for increasing the welding productivity. It utilizes a thin layer of activated flux that brings about an enormous increase in the weld penetration. This outcome is in general, associated with the electrons confinement in the external part of the arc by highly electronegative factors, that restrict the arc creating an effect like that used in plasma welding (Modenesi, Apolinário and Pereira, 2000). Activated flux assisted GTA welding processes are also being explored to take advantage of high penetration which is typically achieved by these processes. The flux assisted processes use common fluxes like oxides, chlorides, flourides fluxes. The flux is usually applied in the form of paste on to the faying surfaces of base metal followed by application of welding arc for melting the base metal. Application of these fluxes results in many desirable effects on the welding a) increasing the arc voltage compared with conventional GTAW or GMAW process under identical conditions of arc length, welding current which in turn burns the arc hotter and leading to an increase in the depth of penetration and b) increasing the constriction of the arc which in turn facilitates the development of weld of high depth to width ratio. Increase in depth of the penetration in turn increases the rate of lateral heat flow from the weld pool to the parent material (K. Devendranath et. al., 2015).

Grade 304L stainless steel is T-300 series. It is "18/8"standard stainless steel mostly found in pans and cooking tools. It is most versatile and widely used alloy in SS family. It has high corrosion Resistance and ease for fabrication. It is also considered to be most weldable high alloy steel and can be welded in all fusion and it has high resistance welding process. Hardness test of 304L stainless steel is 82 in Rockwell B.

2. Literature Survey

Various researchers stated that the difficulties related to the σ-phase and unnecessary grain growth in fusion welding can be controlled by FSW process. A new advancement in TIG welding, that is, A-TIG welding gains popularity among the manufacturers as welding of thick materials can be accomplished in one pass devoid of any edge set up. Studies showed that the penetrating depth can be obtained up to 200% to 300% in A-TIG welding than in traditional TIG welding practice. As studied by Jay J.Vora Vishvesh, J.Badheka (2015), E.Ahmadi and A.R. Ebrahimi(2015), Liming Liu et. al. (2006), activated flux increased the weld penetration mostly due to the existence of surfactant in the pool of the weldment that shifts the surface tension slope and therefore causes a reverse Marangoni pattern of convection that leads to an increased penetration in the weld. Devendranath et al.(2015) made a comparative study using a mixture of multiple fluxes in A-TIG and multi-pass TIG welding of AISI 904L. Results showed that lower values of current A-TIG welding exhibits an enhanced penetration depth. However, the tensile properties of multi-pass TIG welding samples was somewhat greater than the A-TIG welded specimens because of the grain refinement that occurred during multiple passes.

Kuo et al.(2011) stated that, conventional TIG welding formed a smoother and cleaner surface than A-TIG welding. Fluxes used were CaO, Fe_2O_3, Cr_2O_3 and SiO_2 in which SiO_2 generated less

Copyright © 2018 Authors. This is an open access article distributed under the Creative Commons Attribution License, which permits unrestricted use, distribution, and reproduction in any medium, provided the original work is properly cited.

slag where as in case of rest of the fluxes too much slag was obtained. Also the weld morphology in case of TIG welding without flux obtained was broad and superficial where as welding with fluxes showed narrow and deep morphology.

Huang et al. (2006) studied that A-TIG welding can increase the voltage of the arc due to which the heat content in the weld per unit length increases resulting in increase in δ ferrite content in austenitic stainless steel joints. This results in the reduction of chances of hot cracking in the welds. Also an increase in the depth-width ratio of the weld and reduction in HAZ has been noticed which shows the traits of a large level of energy concentrated throughout A-TIG welding, hence the angular distortion of austenitic stainless steel welds can be decreased.

Tseng (2013) noticed an increase in the depth of penetration with the welding current due to the strongly generated arc pressure during TIG welding without flux. Also the penetrating capacity of A-TIG welds increases with the arc pressure. Deep penetration and maximum depth/width ratio of the weld leads to lower angular distortion for A-TIG welds. It occurs because the heat is evenly conducted along the weld thickness.

3. Methodology

3.1. Base Material

The base material AISI 304l stainless steel has been investigated by dry spectroscopic process. The chemical composition obtained is C-0.03%, Mn-2%, Si-0.75%, P-0.045%, S-0.03%, Cr-20%, Mo-3%, Ni-12% and N-10%.

3.2. Various Fluxes Used

The flux was calculated with different weight in Semi Microbalance. The amount of flux is evaluated in Table I. The flux was available in powered form so acetone was added to it to make it semi liquid form. Acetone has a tendency to vaporize quickly leaving behind flux which is applied on the desired area and the brush was moved on the both direction reversed and forward till total flux is applied to the welding area.

Table 1: Flux Weight

Fluxes	IUPAC names of fluxes	Specimen Length(mm)	Specimen width (mm)	Height of the Flux	Density (g/mm^3)	Weight of the flux (g)
SiO_2	Silicon Dioxide	100	3	0.15	0.0025	0.1125
$CdCl_2$	Cadmium chloride	100	3	0.15	0.00405	0.18225

3.4. Welding Set Up

304L stainless steel with thickness 5mm was cut into strips with 100 x 50(mm) then one side of each plate is cut into V groove with the use of angle grinder for good penetration and strength. To calculate the effect of different flux and without use of flux. A-TIG and TIG welding were conducted with Powercon-400A having Power source 10 to 400A. Different welding parameters and levels such as Current, Gas flow rate, Flux weight and flux were changed as shown in Table II. The welding troch with filler rod were moved in welding area and the welding speed with different welding parameters were controlled.

Table 2: Welding Parameters and their levels

Run	Welding Current (A)	Gas rate (l/min)	Flux weight (g)
1	80	10	0.147
2	160	13	0.112
3	200	16	0.187

3.4 Post-Weld Characteristics

After welding, all the samples were taken for mechanical grinding, and polishing to a 0.05μm. Then the sample was etched to a solution of (50ml H_2O + 50ml HCL + 10g $CuSO_4$) and observed under optical microscope. The penetration depth, width of the weld bead and Heat affected Zone was studied. Then multi optimization technique was used to compare both the fluxes and without use of flux and find out the best among it. Hardness of all the specimens was done in Rockwell hardness tester. The reading was studied in B scale. Then the tensile strength was conducted on the weld material.

3.5 Principal Component Analysis (PCA):

For multi-objective optimization of the welding output parameter namely depth of penetration for welding with and without flux, PCA technique is implemented to achieve optimal set of process parameters. The values of the output variables attained during the welding were normalized. The normalized data obtained lies within the range 0 to 1; 1 regarded as the most suitable value and 0 as the least suitable value. The steps of PCA method are illustrated below:

Step-1: The normalized value for 'larger-the-better' and 'smaller-the-better' measure is carried out using eq. (1) and (2):

$$X_a^*(b) = \frac{x_a - [\min(x_a(b))]}{[\max(x_a(b))] - [\min(x_a(b))]} \quad (1)$$

$$X_a^*(b) = \frac{[\max(x_a(b))] - x_a}{[\max(x_a(b))] - [\min(x_a(b))]} \quad (2)$$

where, a = 1,2,.....,i serial no. of experiments
b = 1,2,.....,j output parameters
$X_a^*(b)$= the value of output parameter b after normalization

Step-2: The relation between every pair of quality aspects (j and k) has been scrutinized by using eq. (3).

$$\rho_{bc} = \frac{\mathrm{cov}(Q_b - Q_c)}{\sigma_{Q_b} * \sigma_{Q_c}} \quad (3)$$

where, b= 1,2,.....,m c= 1,2,....,m b≠c
where, ρ_{bc} is correlation coefficient, σ_{Qb} and σ_{Qc} indicates standard deviation of b and c respectively.

Step-3: Evaluation of the principal component score:
a. The calculation of Eigen value λ_c and the comparative Eigen vector β_{cb}c = (1, 2,...m) was done from the correlation matrix generated from all the quality aspects.
b. The principal component scores of the relative series and normalized reference series were computed from eq. (4) as given below:

$$Y_a(c) = \sum_{b=1}^{m} X_a^* \beta_{cb} \quad (4)$$

where, a=0,1,2,....m c= 1,2,.....m
$Y_a(c)$ is the principal component score of the c^{th} factor in the a^{th} sequence. $X_a^*(b)$ is the normalized value of the b^{th} factor in the a^{th} series, and β_c is the b^{th} factor of Eigen vector β_c

Step-4: Estimation of quality loss $\Delta_{0,1}(c)$ is described as the total value of difference between a^{th} experimental value for c^{th} output and the ideal value. It is determined by $[Y_0(c)Y_a(c)]$.

3.6 TOPSIS

The theory of technique for order preference by similarity to ideal solution (TOPSIS) states that the preferred option should have a negligible distance from the positive ideal solution and extreme distance from the negative ideal solution (N. P Senapati, S. Tripathy, S. Samantaray, 2016). The optimal set of data attained by PCA procedure is merged with TOPSIS technique to obtain the optimal parameter set. The steps are illustrated as follows:

Step-1: The principal components obtained in step-4 of PCA method are arranged in the decision matrix form and the input data are set in the manner shown below:

$$D_m = \begin{bmatrix} x_{11} & x_{12} & \dots & x_{1n} \\ x_{21} & x_{22} & \dots & x_{2n} \\ . & . & . & . \\ . & . & . & . \\ . & . & . & . \\ x_{m1} & x_{m2} & \dots & x_{mn} \end{bmatrix}$$

Step-2: Normalized values of decision matrix are obtained using eq. (5):

$$r_{ij} = \frac{X_{ij}}{\sqrt{\sum_{i=1}^{m} {X_{ij}}^2}} \tag{5}$$

where, r_{ij} signifies the normalized value of A_i regarding characteristic X_j.

Step-3: Expanded values of weighted normalized decision matrix, $V=[V_{ij}]$ are determined from eq. (6):

$$V = W_j r_{ij} \tag{6}$$

where, $\sum W_j = 1$

Step-4: The positive and negative ideal solutions are calculated using eq. (7) and eq. (8) respectively.

$$A^+ = \left\{\left(\max v_{ij}, iCj\right), \left(\min v_{ij}, iCj\right)\right\} \tag{7}$$

$$= \left\{v_1^+, v_2^+, \dots \dots v_j^+ \dots . v_n^+\right\}$$

$$A^+ = \left\{\left(\min v_{ij}, iCj\right), \left(\max v_{ij}, iCj\right)\right\} \tag{8}$$

$= \{v_1^-, v_1^-, \dots . v_1^- \dots . v_1^-\}$

Here, j= {1, 2, 3…….n}

Step-5: Every alternative from the ideal solution is accomplished from n-dimensional Euclidean distance that can be calculated using eq. (9) and eq.(10):

$$S_i^+ = \sqrt{\sum_{j=1}^{n} \left(v_{ij} - v_j^+\right)^2} \quad \text{i= 1,2,3, ….n} \tag{9}$$

$$S_i^- = \sqrt{\sum_{j=1}^{n} \left(v_{ij} - v_j^-\right)^2} \quad \text{i= 1,2,3, ….n} \tag{10}$$

Step-6: The comparative closeness to ideal solution is illustrated by eq. (11):

$$C_i^+ = \frac{S_i^+}{S_i^+ + S_i^-} \tag{11}$$

The excellent alternative can be acquired with highest relative coefficient value.

4. Results and Discussion

4.1. Weld Bead Morphology

4.1.1 Penetration

On applying current on SiO_2 flux weldments the depth of penetration gradually increases up to a certain range (i.e, 160A) then the penetration gradually decreases. But while applying Gas flow rate the penetration of the weldments decreases up to a certain flow rate. Flux weight at 0.147 of $CdCl_2$ the penetration is minimum whereas at 0.182gm the penetration was observed to be highest. It was found that the penetration of the weldments are much more higher in using oxide and chloride flux with compared to without use of flux.

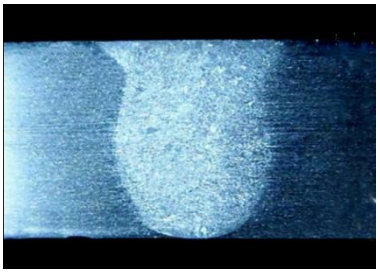

Fig 1: Specimen 16, Weld penetration-5.08mm, Bead width-6.08mm, D/W ratio-0.83

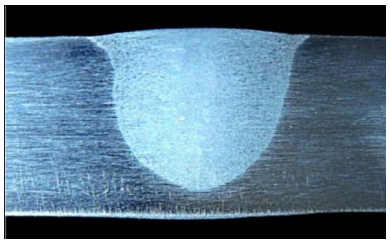

Fig 2: Specimen 8, Weld penetration-4.38mm, Bead width-6.3mm, D/W ratio-0.69

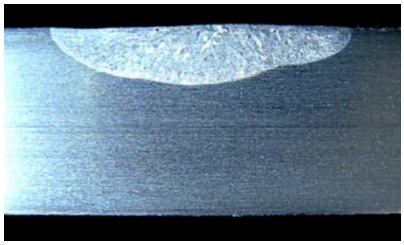

Fig 3: Specimen 3,Weld penetration-2.61mm, Bead width-8.21mm, D/W ratio-0.31

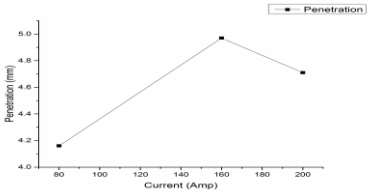

Fig 4: Welding Current vs Penetration of SiO_2

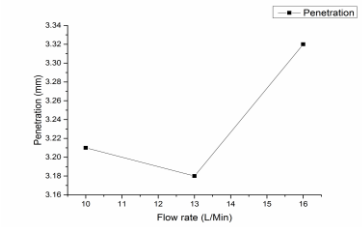

Fig 5: Gas flow rate vs Penetration of without flux

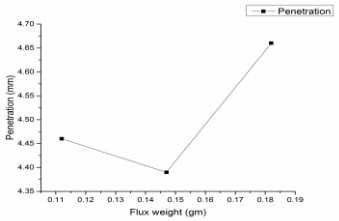

Fig 6: Flux weight vs Penetration of $CdCl_2$

4.1.2 Bead Width

For $CdCl_2$ flux on applying current the increase in the current results to increase in the bead width as because while applying current the temperature of the weldments also increases which result to increase in the bead width (Ajit Khattar, Pawar Kumar, Manish Kumar, 2013) while applying SiO_2 flux the bead width remains constant after the flux weight is 0.147 then their is a gradual decrease in bead width the flow rate of while not using flux the bead width is higher at 13L/Min then the flow rate increases while the bead width decreases. The bead width of the weldments are lower in using oxide and chloride flux with compared to without use of flux.

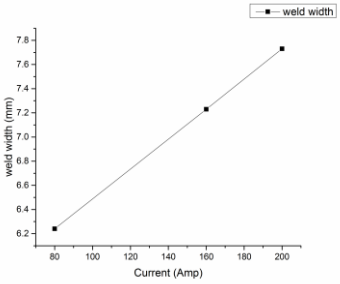

Fig 7: Welding current vs bead width of $CdCl_2$

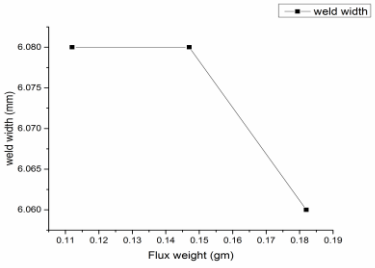

Fig 8: Flux weight vs bead width of SiO_2

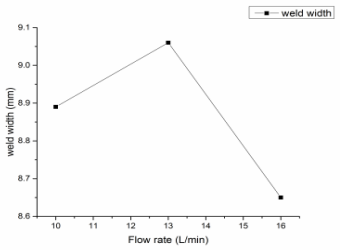

Fig 9: Flow rate vs bead width without flux

4.1.3 Depth/Width Ratio

The increase in welding current increases gradually the depth/width ratio during without use of flux but after 160A of welding their was an sudden increase in depth by width ratio whereas applying Gas flow rate to depth/width ratio the depth /width ratio remains constant till the flow rate attains 13L/Min. Then after their was decrease in depth/width ratio. Flux weight of $CdCl_2$ decreases with an increase in depth/width ratio and vice versa.

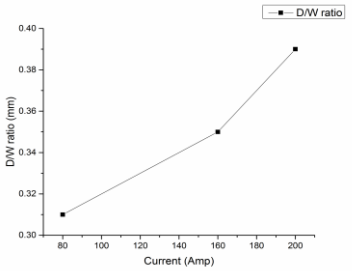

Fig 10: Welding current vs D/W ratio of without flux

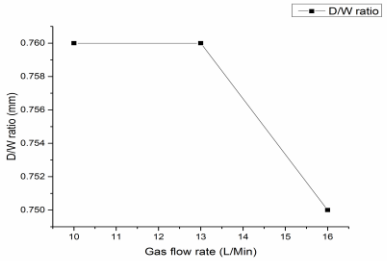

Fig 11: Gas flow rate vs D/W ratio of $CdCl_2$

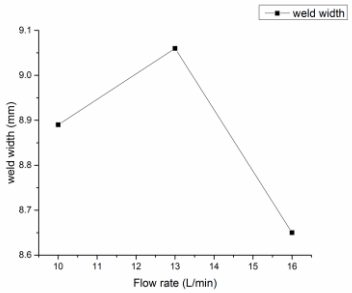

Fig 12: Flux weight vs D/W ratio of SiO_2

4.2 Mechanical Properties of Weldments

4.2.1 Hardness Test

Hardness study shows that the average hardness of the weldments at the joint was higher. The welding current increases the hardness of the weldments at the fusion zone also increases in SiO_2 flux but after 160Aof current the hardness of the fusion zone increases slightly whereas applying flux weight of $CdCl_2$ the hardness of the fusion zone of welding increases in low weight (i.e, 0.112gm) of flux but in case of 0.174gm of flux the hardness of the fusion zone is low and then after increasing in the flux weight there was rise in hardness.

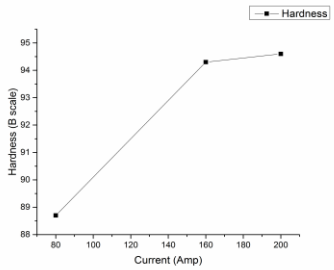

Fig 13: Welding current vs Hardness of SiO_2

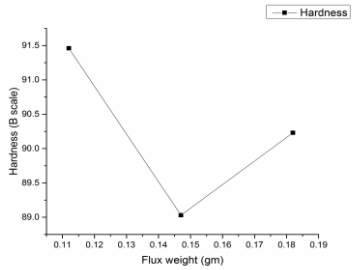

Fig14: Flux weight vs Hardness of $CdCl_2$

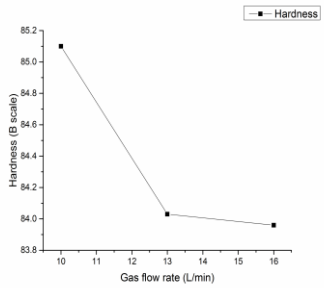

Fig15: Flowrate vs Hardness of without flux

4.2.2 Tensile strength

Tensile strength clearly shows that the failure was occurred in the parent material during TIG welding without flux while failure occurred at the welded joint while using SiO_2 and $CdCl_2$ flux as shown Fig 16. This happens possibly due to the presence of high amount of oxygen and chloride in the weld zone (Ajit Khattar, Pawar Kumar, Manish Kumar, 2013).

Table 3: Tensile Strength Results

Specimens	16	17	18
Elongation Ultimate strength (MPa)	451	545	712
Ultimate Strength (%)	23.1	80.9	80.9
Break Strain (%)	24.8	88.8	88.8
Total time (s)	117	341	448
Offset stress at 0.2% MPa (min)	449	390	389
Offset stress at 0.5% MPa (max)	450	390	392

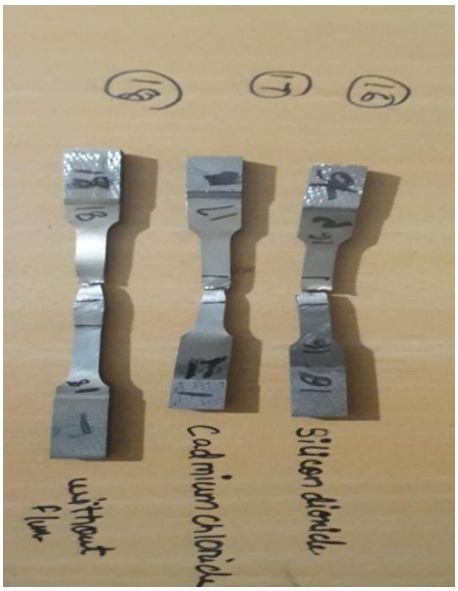

Fig 16: Tensile photograph of 304L stainless steel (16) with use of oxide flux(17) with use of chloride flux(18)with the use of flouride flux

4.3 Microstructure Study

From the study of multi objective optimization result the optimum specimen was found to be SiO_2 flux with current 160A, Gas flow rate 16L/Min and weight of flux 0.147gm so micro structure was studied by optical microscope technique for this specimen. The sample was etched (50ml H_2O + 300ml of HCl + 200ml HNO_3 + 50ml saturated $FeCl_3$ solution + 2.5 g $CuCl_2$). The microstructure of the parent material consists of austentic matix which shows a minor change in the fused area. Whereas their arc constricts due to the presence of oxide flux in weld area.

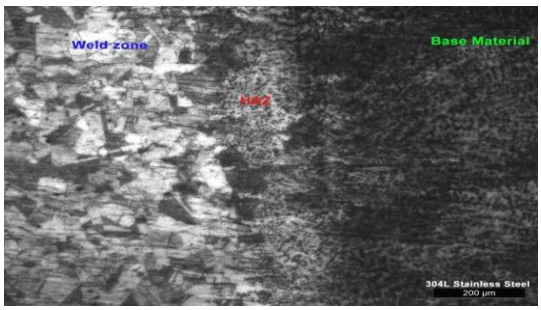

Fig17: Microstructure of base material,weld zone and HAZ

5. Conclusion

The following conclusions drawn from this experimental study are:-

a. SiO_2 flux weldments gives higher penetration with respect to $CdCl_2$ flux and without use of flux with low current and quantity of flux whereas applying greater current of 200 A and 0.182gm of $CdCl_2$ gives higher penetration .
b. There was a greater hardness values while using SiO_2 flux where as using $CdCl_2$ flux and without use of flux their was not much difference in the hardness value with the parent material. But while applying higher Gas flow rate of 16L/min their was a increase in hardness in $CdCl_2$
c. The use of SiO_2 and decreases the bead width with respect to with use of flux. The use of flux reduces the bead width to a limited range. But in case of $CdCl_2$ flux increase in current simultaneously increases the bead width.
d. From the result the optimum specimen was found to be SiO_2 flux with current 160A, Gas flow rate 16L/Min and weight of flux 0.147gm.

e. The failure was occurred at the parent material without use of flux whereas failure occurs at the fusion zone while using SiO_2 and $CdCl_2$ flux.

References

[1] Modenesi PJ, Apolinário ER, Pereira IM. TIG welding with single-componentfluxes. J Mater Process Technol 2000;99:260–5.

[2] K.Devendranath Ramkumar, Aditya Chandrasekhar, Aditya Kumar Singh, Sharang Ahuja, AnuragAgarwal, N.Arivazhagan, Arul Maxiumus Rabel, Comparative studies on the weldabilility ,microstructure and tensile properties of autogenous TIG welded AISI ferritic stainless steel with and without use of flux ,Science direct Volume 20, Part 1, October 2015, Pages 54-69

[3] Jay J.Vora Vishvesh, J.Badheka Experimental investigation on mechanishm and weld morphology of activated TIG welded bead-on-plate weldments of reduced activation ferritic/martensitic steel using oxides fluxes Science direct Volume 20, Part 1, October 2015, Pages 224-233

[4] E.Ahmadi and A.R. Ebrahimi "Welding of 316L austenitic stainless steel with activated Tungsten Inert Gas Process ,Journal of materials Engineering and Performance Volume 24(2),Feb 2015-1065

[5] Liming Liu,Zhaodong Zhang,Gang Song and Yong Shen"Effect of Cadmium Chloride Flux in active Flux TIG welding of Magnesium Alloys" Material Transcation ,Volume 47 (2006)

[6] R.S.Vidyarthy,D.K.Dwivedi "Activating flux tungsten inert gas welding for enhanced weld penetration"Volume 22,Science direct , April 2016, Pages 211-228

[7] Kuo Cheng-Hsien, Tseng Kuang-Hung, Chou Chang-Pin. Effect of activated TIG flux on performance of dissimilar welds between mild steel and stainless steel. Key Engineering Materials 2011;479:74–80.

[8] Huang HY, Shyu SW, Tseng KH, Chou CP. Evaluation of TIG flux welding on the characteristics of stainless steel. Science and Technology of Welding and Joining 2005;10:566–73.

[9] Tsng Kuang-Hung. Development and application of oxide-based flux powder for tungsten inert gas welding of austenitic stainless steels. Powder Technology 2013;233:72–9.

[10] N. Pallavi Senapati, S. Tripathy, S. Samantaray, A Multi-Objective Optimization using a combined approach of Principal Component Analysis and TOPSIS during Electric Discharge Machining of H-11 die steel using P/M processed Cu-Cr-Ni metal matrix composite, International Conference on Electrical, Electronics, and Optimization Techniques (2016)

[11] Ajit khatter, Pawan kumar, Manish Kumar" Optimization of process parameters in TIG welding using Taguchi of stainless steel-304"International Journal of research in mechanical engineering and research, Volume4, Nov 2013